

2016 WSGC Elijah High Altitude Balloon Final Report Team Lake Sharks

Joshua Furey¹, Jared Maraccini¹, Cheyenne Phakousohn¹, Justin Rasmussen², Jonathan Schotte³

¹Milwaukee School of Engineering

²University of Wisconsin Green Bay

³Concordia University Wisconsin

Mission Statement

We are the 2016 Project Elijah Payload team, and we were excited to work on the payload and perform a few experiments. This report details payload design, vegetation health monitoring system, immersive experience, stabilization system, and the air quality system.

Payload Design

Integration of components: The original payload design is basically a cylinder, or tube, that houses all the components. The cylinder includes a sensor and flywheel for the stabilization system within the cylinder along with the air quality sensor system. The infrared and visible SJCAM cameras were placed at the bottom of the cylinder. The two 360° cameras initially were thought to have a better orientation on the side of the payload rather than the top and the bottom, but after testing, the side orientation wasn't as effective. The idea was that the video footage stitching process would be more efficient with this orientation. The concern with placing the cameras on the top and the bottom was the bottom 360° camera would capture the infrared cameras in the footage and vice versa the infrared cameras would capture the 360° camera.

As shown in (Fig. 1), the cylinder was very long in the initial design, around 25 inches long with a 3 inch diameter. However, after testing with the flywheel and the cameras, it was decided to use a different configuration. Instead of a long cylinder, a short and wide cylinder proved to have the best results with a length of 12 inches and a diameter of 6 inches. The team decided to place the 360° cameras in a top-bottom configuration to aid in stitching. Also after much testing with the two camera systems, the top and bottom orientation showed to have a better outcome, specifically based on that the wires from the cameras went into the payload at the bottom and the top. In order for the camera to not interfere with each other, many different setups of the cameras were tested which involved measuring and trigonometry based on each camera's focal viewing angle relative to

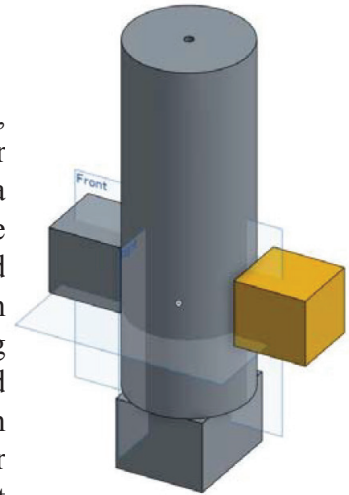


Fig 1: The rugged, initial payload design is shown above with the basic camera orientation.

We would like to thank the Wisconsin Space Grant Consortium and Dr. Farrow for the support on this project.

the horizon of the camera lenses. Each camera required an additional battery pack to run over the duration of the flight, so each camera was wired to a battery pack system within the payload. The team also determined it would be ideal to keep each sub-system separate as much as possible. This would prevent a total-loss, should one fail. As such, each sub-system had its own Arduino microcontroller.

From the initial sketches of the payload, a finalized design was decided on by the team. The team believed this to provide each system with the maximum potential. The payload is best described by separating into its interior and its exterior components.

Interior: The interior design of the payload included a shelf-like stacking of the systems as seen in (Fig. 2). Each system within the payload was mounted to a basswood disc that provided the structure needed to support the components within the payload. The wood discs were mounted to a 12 inch piece of 6 inch diameter rocket blue tube. A semi-circular hatch was sliced out of the tube in order to provide ease of access to the components inside. This design provided the team with enough space to access everything easily while not providing too much unused space. Silicone was used to seal the air quality sensor system, not allowing air to flow through the other compartments of the payload. The reaction wheel system included a flywheel mounted to a wood disc that was mounted to the inside of the body tube. This allowed the flywheel to counteract the spin of the payload.

Exterior: The exterior design of this payload had a cylindrical design as seen in (Fig. 3). This design provided an effective way to best accommodate each subsystem, especially the stabilization system, while maintaining a simple way to build the payload. A cylindrical shell made of polystyrene foam was made to fit securely over the inner tube containing the components. The polystyrene shell was covered with a reflective Mylar to further insulate the inside from reaching levels too cold for the components to operate. Both the vegetative health and immersive system involved mounting cameras to the outside of the payload. The vegetative health system required mounting two cameras to the bottom of the payload where the 360° camera system required a camera on top and bottom of the payload. The payload was sealed shut before launch with 3 aluminum rods

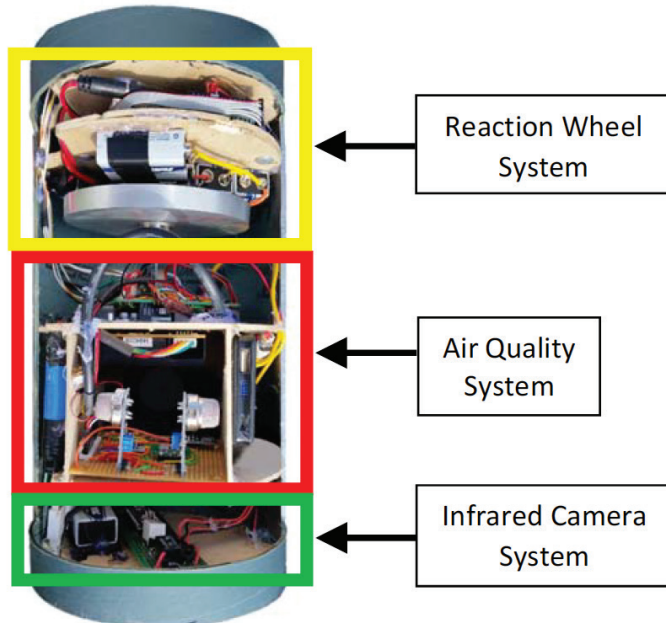


Fig 2: The interior tube and its components are shown, where each independent system mounted to a separate wood disk.



Fig 3: The outer payload shell is shown with the camera systems mounted to the top and bottom.

in the cap, bolted at the top and the bottom, and by spreading silicone over and in holes or seams.

Conclusion: The payload reached 90,000 feet before it began its descent. After retrieving the payload and opening it up to examine the systems, one of the wooden disks had broken. This more than likely was a result of the impact with the payload landed. An improvement could be to use a thicker basswood disk or glue two basswood disks together crossing the grains to add more strength. Ultimately, the outer shell structure of the payload proved to be very strong and provided effective protection to the interior systems.

Monitoring Vegetation Health

Abstract: Is it possible to monitor the health of vegetation using photography? Yes, by taking photos in the visible and infrared spectrum. This section of the report details in-depth how this was accomplished using consumer cameras. With a little post-processing know-how, using photography to capture the health of vegetation brings up some impressive applications and results.

Theory: It is commonly known that most plants are green due to photosynthesis happening in the cellular structure. But how can you tell how healthy it is? By measuring the absorption and reflection of certain wavelengths of light on plants, the health of a plant can be determined. The photosynthetic process absorbs red and blue visible light while reflecting infrared light. The Normalized Difference Vegetation Index (NDVI) formula looks at near infrared light and visible light to calculate the health of the vegetation as seen in (Fig. 4).

$$\left(\begin{array}{c} \text{Near} \\ \text{IR} \end{array} \right) \text{ minus } \left(\begin{array}{c} \text{Red} \\ \text{Green} \\ \text{Blue} \end{array} \right) \\ \text{-----divided by-----} \\ \left(\begin{array}{c} \text{Near} \\ \text{IR} \end{array} \right) \text{ plus } \left(\begin{array}{c} \text{Red} \\ \text{Green} \\ \text{Blue} \end{array} \right)$$

Fig 4: The NDVI formula.

Hardware: Two SJ5000X Elite cameras were used to accomplish this task. These cameras were chosen due to being lightweight and having good photo quality. One of the cameras was modified to take photos in the near-infrared spectrum by removing the infrared light blocking filter and putting a visible light blocking filter in front of the camera. A relay circuit was also made to make the cameras take a synchronized photo every 10 seconds.

Processing: In order for the photos to be worthwhile, they had to be processed. Processing the photos proved to be one of the most challenging aspects of the project. MATLAB was used to process the photos and view results. The MATLAB code used the NDVI formula to construct the image with NDVI values for each pixel.

First the photos needed to be aligned using Photoshop to make sure that each pixel represents the same area on the ground. Then the photos were processed using MATLAB to analyze each pixel individually. In the final NDVI result, the visible light was comprised of the red and blue channels from the visible light photo and the infrared light was the green and blue channels from the infrared camera. The red channel in the infrared photo was tainted by visible light due to the visible light blocking filter so it was not used. The result was an index value that ranged from -1 to +1 with

+1 representing healthy vegetation and -1 representing unhealthy vegetation for each pixel in the resulting photograph.

Results: The results from this experiment turned out great. Using the NDVI formula, there are clear distinctions between healthy vegetation and non-vegetation objects like roads as seen in (Fig. 5). The red, orange, or yellow parts of the photo represent vegetation on the ground. The healthier the vegetation, the more red the color. It is easy to see variations in the health of the vegetation as not all of the vegetation is the same color. One important thing to remember when looking at a NDVI image is that not all vegetation has the same properties. What we mean by this is that different plants absorb and reflect different amounts of visible and near-infrared light. So even though some vegetation may appear healthier, it may not be. More research has to be done on specific types of vegetation in order to compare different vegetation.

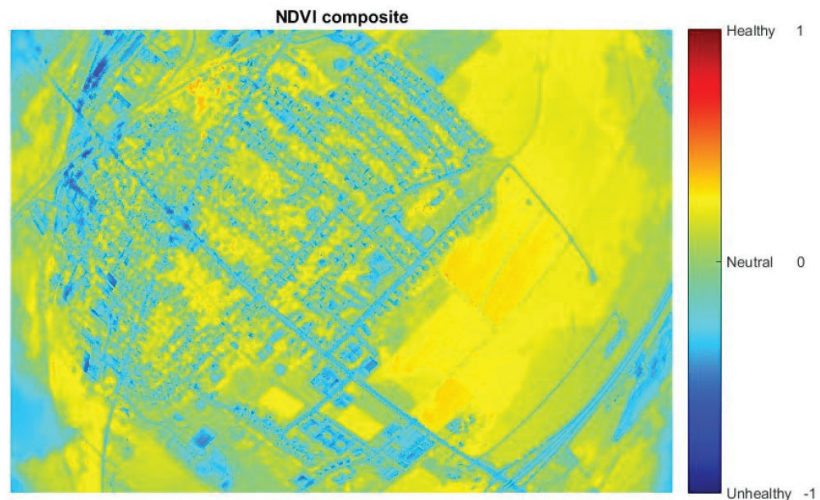


Fig 5: The NDVI resulting image of Clinton, Wisconsin

Conclusion: In conclusion, this experiment was successful and answered the question this experiment sought out to answer. We found that it was possible to measuring the health of vegetation by taking photos in both the visible and near-infrared spectrum. While the greatest benefit of this experiment would come from taking photos of the same area over a period of time, one photograph of the health of vegetation can yield a lot of data.

Immersive Experience

Abstract: Is it possible to create an immersive experience using commercial equipment? Commercial equipment such as the Kodak PIXPRO SP360° 4k and its software help to create 360° videos easier. The goal of implementing the two 360° cameras had partial success, with the top camera recording for 90 min. while the bottom camera recorded for 40 minutes. The visuals recorded by the 360° cameras were stunning, however a completely immersive experience wasn't successful due to the limitations of the technology and its attached software.

Hardware: The team bought two Kodak PIXPRO SP360 4k to create an immersive 360° video of the payload rising with the high-altitude balloon. The team decided to go with the two Kodak PIXPRO SP360 4k because of the features the two cameras offered above their competition. The two cameras weigh a collective 0.6 pounds which is perfect to fit within our weight budget of 6 lbs.

The most important function that the two cameras enabled was the ability to record while having an external battery pack. Many of the 360° cameras advertised were sealed and did not allow

external charging while recording. Our team wanted to record for the full 2 ½ hours of flight that the payload would be experiencing. When looking at possible cameras, either the product had too short of a battery life or the product had the battery life but was too expensive. Some cameras were also not able to handle the more extreme temperature conditions the payload would experience while in flight. The PIXPRO did not have enough battery for the entire flight. In order to extend the battery life of the PIXPRO and to account for the power loss due to cold temperature, an external battery pack was connected to each camera to supply enough power for the entire duration of the flight. Two Google Glass headsets were purchased to view the 360° videos in virtual reality.

Placement on the payload: The team tested various configurations on the payload ranging from keeping the cameras back to back, a top-down camera interface, and a side to side interface. The team decided with a top-down set up on the payload because the stitching of the 360° video along the horizon was easier. The placement of the 360° cameras can be seen in (Fig. 6) below.



Fig 6: The left and right pictures have the top and bottom configuration respectively for the two Kodak PIXPRO SP360 4k camera. The right picture shows the 360° camera placed in between the cameras used for the infrared imaging.

Challenges: The greatest difficulty for the two 360° cameras was the automatic shutoff when the cameras overheated. Testing showed that when the cameras reached approximately 130°F internally, the cameras would automatically shut off. During the battery life testing of the cameras, it was found that in room temperature with no wind conditions the cameras would automatically shut off in about 40 to 60 minutes. This posed a problem because the team wanted to capture the entire flight of the payload, around 90 to 150 minutes. A cold test proved that the camera was still able to function when cooled to -4°F and would be able to capture the entire length of the flight. A cooling fan option was suggested but ultimately not implemented due to finding the issue late in the process of build. The solution found was to mount a large heat sink on the face of the camera with thermal paste. The heat sink enabled dispersion of internal heat produced by the camera. Unfortunately, due to the mount design of the camera, the bottom camera was not able to get as large of a heat sink and could not record the entire flight.

Results: The top camera successfully recorded the full duration of the flight, approximately 90 minutes. The bottom camera recorded for only 40 minutes. It was speculated the camera overheated due to the mounted heat sink not being on the center of the face of the camera and large enough. The creation and stitching of a 360° video was a partial success because the beginning footage for both of the cameras was synced. The failure of the bottom camera and the cameras being out of sync after the 10 minute mark made it difficult to create a seamless stitch for 360° video.

The following videos were shown at the WSGC Superior conference using Google Glass. Highlights of the WSGC Elijah High-Altitude Balloon Launch 2016

<https://www.youtube.com/watch?v=1sEY6XxoLU4>

Immersive 360° video of EBP 2016 Flight

<https://www.youtube.com/watch?v=QAenZdgRBuQ>

Conclusions: Despite the challenges created by overheating, battery life, and software difficulties, the project was successful in yielding immersive footage. The team was able to capture the entire flight with the top camera and half of the flight with the bottom camera. The team was able to stitch the beginning 10 minutes of the flight in immersive 360°. 360° cameras and their software are still in the early stages of development and commercial use is still limited. Overall improvements for the 360° cameras would include making the stitching software more user- friendly and creating a community to share ideas.

Vertical Axis Stabilization

Introduction: The objective of the stabilization system was to determine whether or not a weather balloon's payload can be stabilized enough to record smooth video from an on-board camera. Due to weight restrictions on the payload and the fact that three other experiments were on the same payload, only one axis was attempted to be stabilized. The vertical axis was chosen, because it was resolved to experience the most amount of disturbance. To achieve payload stabilization, a reaction wheel system was pursued.

Background: The most important concept regarding a reaction wheel system is the moment of inertia. Reaction wheels work by spinning a flywheel around the same axis of the spin that is to be counteracted and in the same direction of the object's spin. In essence, the flywheel is spun instead of the object that is to be stabilized. In order to properly counteract the spin of an object, both the object's and the flywheel's moments of inertia need to be known. If the stabilized object feels a force that would cause it to spin at one revolution per minute then the flywheel will have to revolve faster than one revolution per minute to keep the object still (most flywheels have a smaller moment of inertia than the object they are stabilizing and so they have to spin faster). (Eq.1) shows the relationship that an object and its flywheel in a reaction wheel system will have regarding their angular velocities and moments of inertia. Where I represents moment of inertia and ω represents angular velocity.

$$I_1\omega_1 + I_2\omega_2 = 0$$

Eq. 1

Experiment: For the setup of the stabilization system a disk of basswood an eighth of an inch thick with a hole cut in the middle for the motor to be held in vertically. The mount was strengthened by adding a custom machined plastic piece around the motor to spread the stresses caused by the reaction wheel across the wooden disk more evenly. The motor was oriented so that the output shaft was pointed downward with the flywheel attached. This allowed enough clearance between the flywheel and the wood disk for five 9V batteries to be mounted on the underside of the disk. Two pairs of 9V batteries connected in series were connected in parallel together to provide 18 volts to the motor with an ample battery life. An Arduino Uno, LSM6 gyroscope, and LISMD3L motor controller were all attached to the top of the disk. One nine-volt battery powered both the Arduino Uno and gyroscope. The batteries were connected to their components through a partial circle cut in the side of the wood disk. (Fig. 7) shows a side, top, and bottom (from left to right) views of the stabilization system.



Fig 7: Side, Top, and Bottom Views of the Stabilization System.

Results: Unfortunately, no direct data from the gyroscope was recorded as the Arduino Uno could not support the LSM6 gyroscope and an Arduino SD shield. The SD shield would have been used to directly record data from the gyroscope onto a micro SD card. An Arduino Mega has the capability to handle both the gyroscope and the SD shield, but would not have fit in the space allocated inside the payload for the stabilization system. The team decided not to attempt a design modification to allow the use of a Mega as the payload was already very near its maximum design limits. Alternatively, the effectiveness of the stabilization was determined by the video footage taken by the 360° degree camera videos and also by using their audio. Audio from the cameras proved valuable as it granted knowledge of whether or not the motor was operating at any given time. This qualitative data helped in the analysis of determining when and why the stabilization system ceased working during the flight. Similarly, the video provided direct feedback to the effectiveness of the reaction wheel since the goal was to keep the camera from spinning as much as possible. Overall, the reaction wheel system achieved less than satisfactory, yet promising results. The stabilization system decreased the spin experienced by the camera and after analysis of how it performed in flight the system shows potential for improvements to greatly minimize payload spin.

Conclusion: Overall, the project produced unsatisfactory results for the team. The payload's spin around the vertical axis was not controlled as much as expected. Also, the system's housing and mounting was overlooked in the design phase and did not handle all of the stresses during flight. However, the project did show a great amount of promise. The team strongly believes that the design and system chosen could meet all expectations with modifications in the system coding, component mounting, and power system.

Air Quality Sensor Array

Abstract: Air quality is an ongoing concern, as humans continue to manufacture and pollute our planet. The purpose of this experiment was to identify if an affordable sensor array that would have the ability to provide accurate air quality data during the ascent of the balloon. We were able to record some excellent data during the flight, while also narrowing down viable sensors for future payloads.

Initial Research: We used data from the NASA's own Goddard Earth Science website to determine the critical indicators to be measured. This then led to a trying search for a proper set of sensors that were within our budget, while measuring the required ranges. Many of the sensors available for air quality are designed for usage in residential and commercial locations. While these sensors would work for low-altitude conditions, they lacked the ability to read trace values.

Hardware: An Arduino Mega was the chosen microprocessor for this application. It allowed for a wide selection of inputs and outputs, while offering more memory for software. The following were the selected sensors, as they met our price point while providing adequate operating ranges. We were unable to use electrochemical sensors in this project due to cost.

- Ozone - 2x SainSmart MQ131
- Particulate - DSM501A
- Temperature/Pressure/Altitude - BMP180
- Ultraviolet - Waveshare UV Module
- Display - Generic .96" OLED
- Nitrogen Dioxide - SGX Sensortech MICS-2714
- Volatile Organic Compounds - SGX Sensortech MICS-VZ-89
- Carbon Monoxide - SGX Sensortech MICS-5524

Challenges: One of the largest drawbacks was the lack of I2C ports on the Arduino Mega. While the Mega has two ports, rather than one on a typical Arduino module, this was a large hurdle to overcome. This issue was fully realized by the third week of the project, as we began to pare the sensor list down. However, it proved to be a long-term hurdle. This led us to choosing analog based sensors, which provided their own set of challenges. The analog MICS sensors from SGX proved to be the most challenging. We later ordered a Pulse-Width Modulation (PWM) module with the same MICS sensor to circumvent these issues. However, the Arduino platform proved to have even more problems measuring PWM. The manufacturer offered I2C options, but our I2C ports were occupied with the display and SD card module. The display was needed to ensure proper function during pre-flight, and the SD module was required for data recording. A microcontroller with a multitude of I2C ports is a recommendation for future teams.

The environment also proved to be a significant challenge. All of our air quality sensors relied on a small heating element to function. As temperature fluctuates, so do the readings from the sensors. Thankfully, our ground-level vacuum and freeze testing provided calibration readings to adjust for temperature fluctuation. Our particulate sensors had similar environmental challenges. We worked with two different units during testing and found both to have very particular ambient requirements. Each sensor required minimal airflow, which proved to be very difficult to accomplish in our

tightly-packed payload.

Results: With our data adjusted for proper temperature fluctuation, we were able to determine very similar ozone abundances to data provided by the National Oceanic & Atmospheric Administration (Ozone in the Atmosphere) as seen in Figure 8. The decision to fly two identical ozone sensors proved to be wise. While the sensors output similar data, one provided more finite measurements come flight day. Our Ultraviolet sensor also provided data that closely matched predictions by the World Health Organization (WHO) as seen in Figure 9. Per the WHO, UV levels increase by 10% to 12% every 1000 meters (Ultraviolet radiation and health). Our sensor provided readings that indicated 8% to 20% increase per 1000 meters. In Figure 9 the magenta line shows altitude, while the blue line indicates UV readings over the course of the flight. The vast jumps in data were caused by the sway of the payload during flight. Unfortunately, the CO data did not collect proper data during the flight. We were unable to determine the cause of the failure, but believe it was related to an electrical failure that occurred during launch prep. While the data measured from these sensors looked hopeful, careful review proved that it was simply analog noise. The particulate sensor provided data, but the values were far too inconsistent to create a conclusion. Upon review, we believe there was an insignificant amount of airflow through the sensor.

Conclusion: While we had some difficulties with our configuration, we sought out to accomplish a difficult goal with a limited budget. The lack of electrical engineering knowledge was our largest setback for this experiment.

With more knowledge and time, much more debug and testing could have been done. We did recover some excellent data, while also providing insight for future teams.

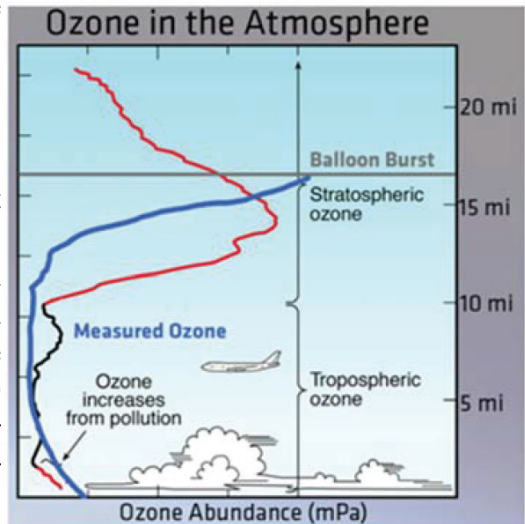


Fig 8: Measured Ozone Abundance

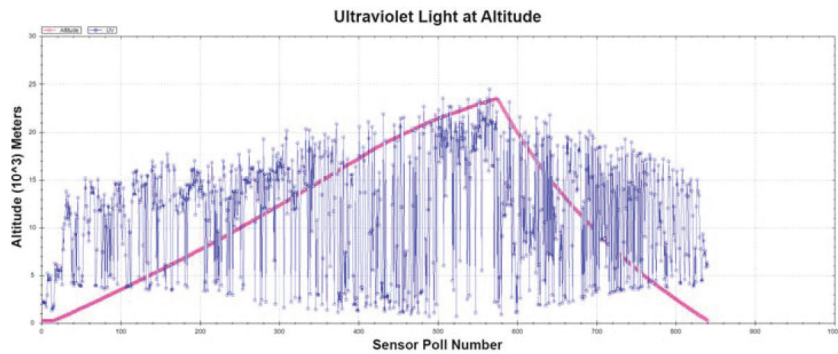


Fig 9: Measured Ultraviolet Light at Altitude.

References

2015. AN4682 Application note LSM6DS33: always-on 3D accelerometer and 3D gyroscope. pololu.com. Retrieved from <https://www.pololu.com/file/0J1088/LSM6DS33-AN4682.pdf>
2015. LSM6DS33 iNEMO inertial module: always-on 3D accelerometer and 3D gyroscope Datasheet. pololu.com. Retrieved from <https://www.pololu.com/file/0J1087/LSM6DS33.pdf>
2016. 6.7.1. Arduino Examples. pololu.com Retrieved from <https://www.pololu.com/docs/0J44/6.7.1>
- kevin-pololu. 2016. MinIMU9AHRS.ino. pololu.com. Retrieved from <https://github.com/pololu/mini-9-ahrs-arduino/blob/master/MinIMU9AHRS/MinIMU9AHRS.ino>
- Normalized Difference Vegetation Index Formula. (n.d.). Retrieved June 21, 2016, from <https://publiclab.org/wiki/ndvi>
- Ozone in the Atmosphere [Digital image]. (n.d.). Retrieved September 5, 2016, from <http://www.esrl.noaa.gov/csd/assessments/ozone/2010/twentyquestions/images/Q1-2.jpg>
- Ultraviolet radiation and health. (n.d.). Retrieved September 7, 2016, from http://www.who.int/uv/uv_and_health/en/